

Compared to the bis(metal) phosphinidenes, **1** probably does not enjoy any substantial stabilization from $\pi\text{p}-d\pi$ interactions.^{10,19-23} The weak Ag-P interaction and the close P-O interaction (as in free ADPO) indicate the preference for the hypervalent bonding arrangement over $\text{Ag} \rightarrow \text{P}$ back-bonding. Also, as observed previously, ADPO does not form pnictinidene-like complexes with $\text{CpMn}(\text{CO})_2$ fragments as do the heavier members of the ADPO series.¹⁰

Attempts are currently under way to isolate monomeric $\text{ADPO}[\text{Ag}^+(\text{CH}_3\text{CN})_3]_2(\text{SbF}_6^-)_2$ (**2**), and other metal complexes of planar ADPO. Preliminary data indicate the formation of **2**

in solution, but attempted crystallization lead to the formation of **1** and $\text{Ag}^+(\text{CH}_3\text{CN})_4\text{SbF}_6^-$.

Acknowledgment. The excellent technical assistance of Hugh A. Craig and William J. Marshall made this work possible. Fredric Davidson kindly provided the NMR spectroscopic results reported herein.

Supplementary Material Available: A complete description of the X-ray crystallographic structure determination on **1** including a description of the experimental procedures, tables of fractional coordinates and isotropic thermal parameters, anisotropic thermal parameters, and distances and angles, and ORTEP structure drawings (7 pages). Ordering information is given on any current masthead page.

- (19) Arif, A. M.; Cowley, A. H.; Norman, N. C.; Orpen, A. G.; Pakulski, M. *Organometallics* **1988**, *7*, 309.
 (20) Huttner, G.; Borm, J.; Zsolnai, L. *J. Organomet. Chem.* **1984**, *263*, C33.
 (21) Huttner, G.; Evertz, K. *Acc. Chem. Res.* **1986**, *19*, 406.
 (22) Bartlett, R. A.; Dias, H. V. R.; Flynn, K. M.; Hope, H.; Murray, B. D.; Olmstead, M. M.; Power, P. P. *J. Am. Chem. Soc.* **1987**, *109*, 5693.
 (23) Lang, H.; Orama, O.; Huttner, G. *J. Organomet. Chem.* **1985**, *291*, 293.

Du Pont Central Research and Development
 Experimental Station
 Wilmington, Delaware 19880-0328

Anthony J. Arduengo, III*
 H. V. Rasika Dias*
 Joseph C. Calabrese

Received September 12, 1991

Articles

Contribution from the Department of Chemistry, Faculty of Pharmacy & Biochemistry, University of Zagreb, 41000 Zagreb, Croatia, Yugoslavia

Siderophore Chemistry of Vanadium. Kinetics and Equilibrium of Interaction between Vanadium(IV) and Desferrioxamine B in Aqueous Acidic Solutions[†]

Ines Batinić-Haberle, Mladen Biruš,* and Marijan Pribanić

Received July 3, 1991

The kinetics and equilibrium of interaction between vanadyl sulfate and a natural trihydroxamate-based siderophore, desferrioxamine B methanesulfonate, were studied spectrophotometrically in acidic aqueous perchlorate solutions of 2.0 M ionic strength. The bi-, tetra-, and hexadentate-bonded complexes were formed under these conditions, and their stability constants were calculated. The rate constants for the formation and hydrolysis of the bi- and tetradentate complexes were estimated. The formation of the bidentate complex proceeds via two parallel pathways involving the hydrolyzed and unhydrolyzed vanadyl-aquo species. The hydrolyzed form was found to react with the siderophore ca. 10^5 times faster than the unhydrolyzed form.

Introduction

Numerous living organisms are capable of selectively concentrating various trace elements against an extreme concentration gradient due to the participation of low molecular weight molecules that are involved as the carriers. Tunicates, a certain type of sessile marine organism, are for example known to concentrate vanadium 10^8 -fold over the sea water level of ca. 0.1 ppb.¹ Although vanadium is the principal metal stored in the vanadocytes, iron was also found to be present as a constituent.^{2,3} A possible common mechanism for transport and storage of these two metals was considered, since in human organisms the same proteins appear to be involved with both metals.⁴ Although during the last two decades the chemistry of vanadium attracted great interest, the biochemical role of this essential trace element is still poorly understood compared to the other first-row transition metals.⁵ Its eventual better understanding, at least in part, depends on our understanding of the coordination chemistry of vanadium in its different oxidation states.

In a previous communication⁶ we have reported on the mechanism of the interaction between VO_2^+ ion and desferrioxamine B in strongly acidic medium. Desferrioxamine B, $\text{NH}_2(\text{CH}_2)_5\text{-}\{\text{N}(\text{OH})\text{C}(\text{O})(\text{CH}_2)_2\text{C}(\text{O})\text{N}(\text{H})(\text{CH}_2)_3\}_2\text{N}(\text{OH})\text{C}(\text{O})\text{CH}_3 = \text{H}_3\text{DFB}$, is a linear trihydroxamate-based siderophore produced by certain microorganisms⁷ and besides iron(III) also very strongly chelates vanadium ions.^{6,8,9} This siderophore is currently used as a drug in the treatment of patients suffering from Cooley's

anemia¹⁰ or chronic dialysis.¹¹ Therefore, the obtained results may be of some relevance in predicting a potential disturbance in the vanadium balance in these patients as a consequence of the administration the drug. Hence, it seemed worthwhile to undertake a study of the interaction between vanadium in its 4+ oxidation state and desferrioxamine B, the results of which are presented in this report. Apart from their eventual biological application, the results throw some more light on the intimate mechanism of the substitution reactions at the V(IV) metal ion center. Besides the new kinetic data on this system, our results also augment a previous study⁸ regarding the equilibrium constants of the system, which has been published during the preparation of this paper.

- (1) Kustin, K.; McLeod, G. C. *Struct. Bonding (Berlin)* **1983**, *53*, 140.
 (2) Swinehart, J. H.; Biggs, W. R.; Halko, D. J.; Schroeder, N. C. *Biol. Bull. (Woods Hole, Mass.)* **1974**, *146*, 302.
 (3) Macara, I. G.; McLeod, G. C.; Kustin, K. *Comp. Biochem. Physiol., B: Comp. Biochem.* **1979**, *638*, 299.
 (4) Marafante, E.; Sabbioni, E. In *Manage Control Heavy Metal Environment*; CEP Consultants LTD.: Edinburgh, U.K., 1979, p 171.
 Chasten, N. D.; Theil, E. C. *J. Biol. Chem.* **1982**, *257*, 7672. Chasten, N. D. *Struct. Bonding* **1983**, *53*, 105.
 (5) Boyd, D. W.; Kustin, K. *Adv. Inorg. Biochem.* **1984**, *6*, 312.
 (6) Batinić, I.; Biruš, M.; Pribanić, M. *Croat. Chem. Acta* **1987**, *60*, 279.
 (7) Neilands, J. B., Ed. *Microbial Iron Metabolism*; Academic Press: New York, 1974.
 (8) Keller, R. J.; Rush, J. D.; Grover, T. A. *J. Inorg. Biochem.* **1991**, *41*, 269.
 (9) Luterotti, S.; Grdinić, V. *Analyst* **1986**, *111*, 1163.
 (10) Anderson, W. F.; Bank, A.; Zaino, E. C., Eds. Fourth Cooley's Anemia Symposium. *Ann. New York Acad. Sci.* **1980**, *344*, 375.
 (11) Ackrill, P.; Ralston, A. J.; Day, J. P.; Hodge, K. C. *Lancet* **1980**, *2*, 692.

[†] Taken in part from I.B.-H.'s Ph.D. Thesis.

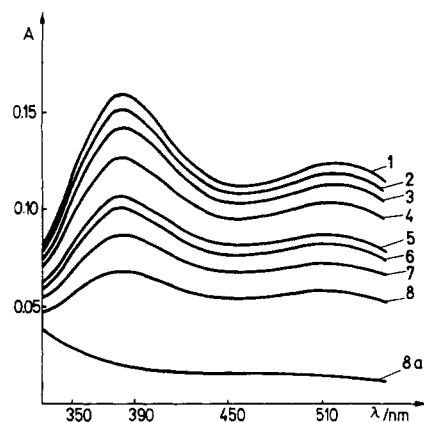


Figure 1. Electronic spectra of the equilibrated solutions of 40 μM VOSO_4 and 0.4 mM desferrioxamine B at 25 $^\circ\text{C}$ and 2.0 M ionic strength (perchlorate). The concentration of HClO_4 is as follows: (1) 10 mM; (2) 1.04 mM; (3) 0.48 mM; (4) 0.2 mM; (5) 80 μM ; (6) 56 μM ; (7) 24 μM ; (8) no added HClO_4 ; (8a) pH = 6.

Experimental Section

Materials. All solutions for kinetic and equilibrium studies were prepared in water, which was doubly distilled from alkaline permanganate in an all-glass apparatus. The solutions of desferrioxamine B (Ciba, Desferal) were prepared by weight from the recrystallized methanesulfonate salt (methanol, mp 149 $^\circ\text{C}$, uncorrected) and used the same day. The solutions of vanadyl sulfate were prepared by weight of the solid (Aldrich, 99.999%) kept in a vacuum desiccator over P_4O_{10} or prepared by reduction of V_2O_5 (Riedel, pa) with SO_2 .¹² The solutions were standardized by potentiometric titration against KMnO_4 .¹³ The ionic strength of 2.0 mol dm^{-3} was maintained by the addition of NaClO_4 , recrystallized from water, standardized by exchange on Dowex 50W-X8 (H^+) cation-exchange resin and titration with NaOH .

Equilibrium Measurements. Solutions of vanadyl sulfate in Na/HClO_4 were mixed with the ligand solutions in the same medium, and absorbance of the 510-nm band was recorded on a Pye Unicam 8-100 or a Perkin-Elmer Model Lambda-3 spectrophotometer equipped with a thermostated cell holder. At 25 \pm 0.1 $^\circ\text{C}$ the absorbance quickly rises to a maximum and then very slowly decreases due to decomposition of desferrioxamine B in strongly acidic solutions. Proton concentrations of equilibrated solutions were calculated by summing up added acid and protons released during complexation.

Kinetic Measurements. Kinetic experiments were carried out on Durrum D-110 stopped-flow and a Perkin-Elmer Lambda-3 UV-vis spectrophotometers thermostated at 25 \pm 0.1 $^\circ\text{C}$. Two types of experiments were performed. In the first, the solutions of vanadyl sulfate and desferrioxamine B, in the same medium, were mixed together in the instrument and the increase in absorbance was followed at several different wavelengths. In another series of kinetic runs, equilibrated solutions containing vanadyl sulfate and desferrioxamine B at $\text{p}[\text{H}^+] \geq 4$ were mixed in the stopped-flow instrument with solutions of different acidity. The increase in absorbance and its eventual decrease at 510 nm were monitored. All the solutions were of 2.0 M ionic strength. In most of the runs, pseudo-first-order conditions were ensured by keeping one of the reactants at a much lower concentration than the others. Under these conditions the rate constants were therefore calculated by fitting the data points to the equation $A_t = A_0 e^{-kt} + A_\infty$, where the A symbols have the usual meaning of absorbance at different times t . When the pseudo-first-order conditions were not met since the total concentrations of the VO^{2+} and H_4DFB^+ ions during the formation kinetics were equal, the observed forward rate constants were calculated by fitting the absorbance data points to the equation

$$A_t = \epsilon m_1 m_2 \{1 - \exp[kt(m_1 - m_2)]\} / \{m_2 - m_1 \exp[kt(m_1 - m_2)]\}$$

where ϵ is the apparent molar absorbance coefficient of the equilibrated solutions. The parameters m_1 and m_2 represent $a + 0.5K^{-1} \pm (aK^{-1} + 0.25K^{-2})^{1/2}$, where a represents the initial concentration of both the vanadyl ion and the ligand and K is an apparent equilibrium constant in each of the runs. When the hydrolysis of the produced complex was followed in the absence of an excess of any of the reactants, the forward

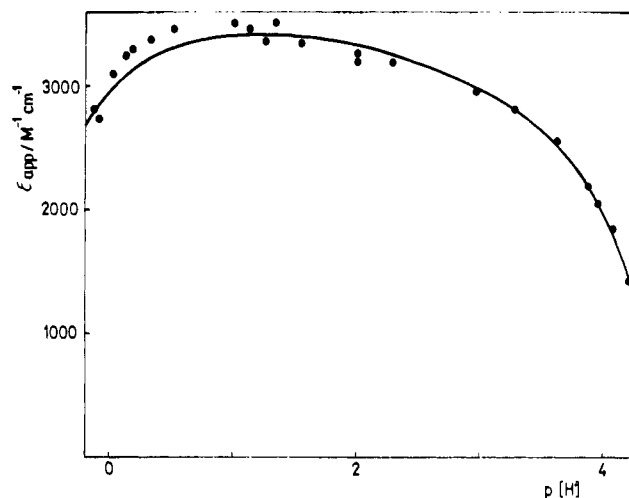


Figure 2. Dependence of the absorbance at 510 nm of the equilibrated solutions of 50 μM VOSO_4 and 0.5 mM desferrioxamine B on $\text{p}[\text{H}^+]$ at 25 $^\circ\text{C}$ and 2.0 M ionic strength (perchlorate).

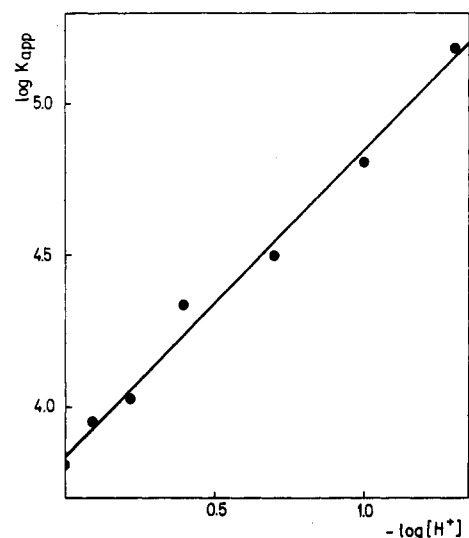


Figure 3. Dependence of the apparent equilibrium constant (for definition see the text) on $\text{p}[\text{H}^+]$. Experimental conditions: $[\text{VOSO}_4] = 0.1$ mM; $[\text{desferrioxamine B}] = 50\text{--}400$ μM ; at 25 $^\circ\text{C}$; 2.0 M ionic strength (perchlorate); at 510 nm.

rate constants of the hydrolysis were calculated by fitting the absorbance data points to the equation $A_t = A_0(A_\infty + A_0E)/(A_0 + A_\infty E)$, where $E = \exp[-(A_0 + A_\infty)kt/(A_0 - A_\infty)]$.

Other Measurements. IR spectra were recorded on a Perkin-Elmer M-547 grating spectrometer as KBr pellets.

ESR spectra were recorded on a Varian E-109 spectrometer, at 77 K in liquid nitrogen, with diphenylpicrylhydrazyl radical (DPPH) as a g marker ($g = 2.0037$).

A Radiometer PHM85 pH meter was used for pH measurements in neutral and weakly acidic solutions.

A nonlinear least-square curve-fitting program based on the published routines¹⁴ was used for all the calculations performed on a Compaq Deskpro 386s computer.

Results

Equilibrium Measurements. According to Keller et al.⁸ two different vanadyl-desferrioxamine B complexes are formed in acidic aqueous solutions. Figure 1 presents electronic spectra of the equilibrated solutions of vanadyl sulfate and desferrioxamine B as a function of the perchloric acid concentration, which con-

(12) Brauer, G. *Handbook of Preparative Inorganic Chemistry*, 2nd ed.; Academic Press: New York, 1965; Vol. 2, p 1258.

(13) Vogel, A. I. *Textbook of Quantitative Inorganic Analysis*, 2nd ed.; Longmans, Green and Co.: London-New York-Toronto, 1953; p 319.

(14) Sharma, V. S.; Leussing, D. L. *Talanta* 1971, 18, 1137. Bevington, P. R. In *Data Reduction and Error Analysis for the Physical Sciences*; McGraw-Hill, Inc.: New York, 1969.

(15) Schwarzenbach, G.; Schwarzenbach, K. *Helv. Chem. Acta* 1963, 46, 1390.

(16) Rossotti, F. J. C.; Rossotti, H. S. *Acta Chem. Scand.* 1955, 9, 1177.

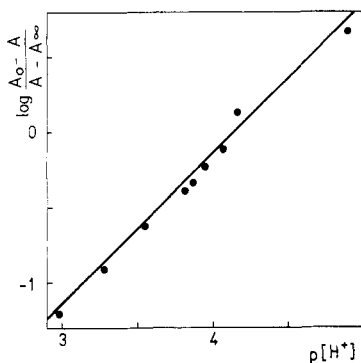
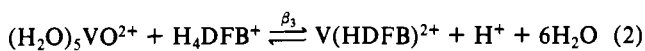
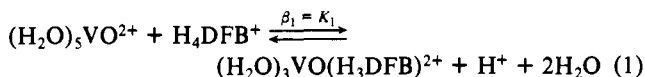


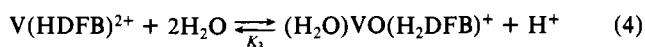
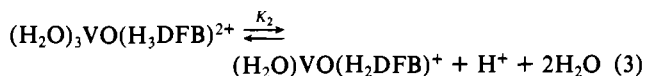
Figure 4. Hill's plot for the interaction of 0.1 mM VOSO_4 and 0.1 mM desferrioxamine B at 25 °C, 2.0 M ionic strength (perchlorate), and 510 nm.

firmly those findings.⁸ The first complex exhibits strong bands at 385 and ca. 515 nm (a broad maximum), and the other one has its bands shifted to the shorter wavelengths of the UV spectrum. Job's method of continuous variations of the metal and ligand concentrations revealed that at 0.1 and 0.01 M proton concentrations the formed complexes are 1:1 in metal to ligand ratio. A plot of the absorbance at 510 nm versus $\text{p}[\text{H}^+]$ exhibits a bell-shaped curve, as shown in Figure 2, which indicates dissociation of at least two protons during complexation. In strongly acidic solutions, $[\text{HClO}_4] \geq 0.05 \text{ M}$, a plot of $\log K_{\text{app}}$ versus $\text{p}[\text{H}^+]$ gives a straight line, as shown in Figure 3, with a calculated slope of 1.01 (5) (hereafter numbers in parentheses represent the single value of standard deviation expressed in terms of the last significant digits reported for the parameter). K_{app} is defined as the equilibrium concentration of the formed complex divided by the product of the equilibrium concentrations of the uncomplexed metal ion and ligand. From the obtained slope it may be concluded that in the first complexation equilibrium only one proton is released. The number of protons released in the second equilibrium stage was determined from the slope of Hill's plot under the experimental conditions that the fraction of uncoordinated vanadyl ion is low enough to be neglected. Figure 4 demonstrates the linearity of $\log \{(A_0 - A)/(A - A_\infty)\}$ vs $\text{p}[\text{H}^+]$, with a calculated slope of 1.00 (4). This suggests that in the second equilibrium one proton is released as well.

Therefore, overall two protons per vanadyl ion are released during the two-stage coordination of H_4DFB^+ . From the reported ligand¹⁵ and vanadyl¹⁶ acid dissociation constants it can be predicted that the uncoordinated ligand is in the fully protonated form, H_4DFB^+ (the ligand terminal amino group also being protonated), whereas the "uncoordinated" metal ion is mainly in the $(\text{H}_2\text{O})_5\text{VO}^{2+}$ form. The observed release of one proton in the first equilibrium may correspond to the formation of bi- and/or hexadentate complexes described by eqs 1 and 2. The observed



release of the second proton may be described by eqs 3 and 4. A



noteworthy aspect of the proposed scheme is that increasing acidity will favor the hexa- over the tetradentate form of the complex (eq 4), which is in contrast to the behavior of the majority of coordination complexes of transition-metal ions with monoprotic ligands. The reason for this is that coordination of the third hydroxamic acid of desferrioxamine B is accomplished by dissociation of *one* proton, during which the expelled oxo ligand in solution binds *two* protons.

Table I. Equilibrium and Kinetic Parameters (Defined in Text) for the Desferrioxamine B–Vanadium(IV) Interaction at 25 °C and 2 M Ionic Strength (NaClO_4)

K_I	$6.24 (28) \times 10^3$	$k'_1 K_h$	$2.55 (35) \text{ s}^{-1}$
	$6.60 (76) \times 10^3$ ^a	k_{-1}	$9.0 (23) \times 10^{-1} \text{ M}^{-1} \text{ s}^{-1}$ ^b
K_{II}	$5.98 (36) \times 10^{-5} \text{ M}$		$8.5 (18) \times 10^{-1} \text{ M}^{-1} \text{ s}^{-1}$ ^c
K_1	$1.87 (50) \times 10$	k'_{-1}	$1.36 (47) \times 10^{-1} \text{ s}^{-1}$ ^d
K_2	$1.99 (41) \times 10^{-2} \text{ M}$		$6.6 (25) \times 10^{-1} \text{ s}^{-1}$ ^e
K_3	$1.67 (40) \times 10^4 \text{ M}^{-1}$	k_2	$1.03 (12) \times 10 \text{ s}^{-1}$
k_1	$1.69 (14) \times 10 \text{ M}^{-1} \text{ s}^{-1}$	k_{-2}	$5.17 (62) \times 10^2 \text{ M}^{-1} \text{ s}^{-1}$

^a Calculated from the kinetic data, $K_I = (\text{slope of Figure 6})/(\text{slope of Figure 7})$. ^b Calculated from the formation data, $k_{-1} = k_1/K_I$. ^c Calculated from the hydrolysis data, $k_{-1} = (\text{slope of Figure 7})(1 + K_2 K_3)$. ^d Calculated from the formation data, $k'_{-1} = k'_1 K_h / K_I$. ^e Calculated from the hydrolysis data, $k'_{-1} = (\text{intercept of Figure 7})(1 + K_2 K_3)$.

If we neglect the number of released water molecules during the complexation reactions, an equilibrium constant for the first complexation step may be written as indicated in (5), and an equilibrium constant for the second complexation step may be written as given in (6).

$$K_I = \frac{\{[(\text{H}_2\text{O})_3\text{VO}(\text{H}_3\text{DFB})^{2+}] + [\text{V}(\text{HDFB})^{2+}]\}[\text{H}^+]}{[(\text{H}_2\text{O})_5\text{VO}^{2+}][\text{H}_4\text{DFB}^+]} \quad (5)$$

$$K_{II} = \frac{[(\text{H}_2\text{O})\text{VO}(\text{H}_2\text{DFB})^+][\text{H}^+]}{[(\text{H}_2\text{O})_3\text{VO}(\text{H}_3\text{DFB})^{2+}] + [\text{V}(\text{HDFB})^{2+}]} \quad (6)$$

All the measured spectrophotometric data points were fitted to eqs 5 and 6 by means of the nonlinear curve-fitting procedure. The evaluated values of K_I and K_{II} are listed in Table I.

The vanadyl species in reaction mixtures of lower acidity ($[\text{H}^+] < 10^{-4} \text{ M}$) spontaneously oxidize in the presence of air (oxygen), whereas under strictly anaerobic conditions the equilibrated solutions were found to be stable. In most of the experiments the oxidation process was however slow enough to not interfere significantly with the substitution reactions at the metal ion center. ESR spectra of the equilibrated reaction solutions of various acidities exhibit characteristic features for V^{4+} species.⁸

Keller et al.⁸ presented ESR evidence for the domination of the hexadentate over bidentate complex in the first equilibrium. In order to prove it, an attempt was made to isolate solid complexes by vacuum evaporation of the reaction mixtures at different acidities in dinitrogen atmosphere. IR spectra of the dried material differ from the spectra of the uncomplexed ligand and the metal ion exhibiting a band at 935 cm^{-1} , which is characteristic for the $\text{V}=\text{O}$ bond in oxovanadyl complexes.^{17–19} An absence of this band would be indicative of the hexadentate complex that should have all six coordination sites of the vanadium(IV) metal ion center occupied by the hydroxamate donor atoms. In the spectrum of the material isolated from the more acidic solutions (proton concentration $\geq 10^{-3} \text{ M}$), the 935-cm^{-1} band is much weaker than that in the material isolated from the solutions of lower acidity. Therefore, the observed IR spectra confirm the model in which the first complexation step results in the predominant formation of the hexadentate complex, whereas the second step mainly represents a proton equilibration of the hexa- and tetradentate complexes. These observations are also in agreement with recently reported data for the vanadyl–rhodotolurate complex,²⁰ which electronic spectra exhibited maxima at 390 and 516 nm and were assigned to the hexadentate species precipitated from the solution.

Although collected spectrophotometric data make possible a very accurate calculation of the equilibrium constants K_I and K_{II} , they are not sufficient for the calculation of an equilibrium

(17) Evans, J. C. *Inorg. Chem.* **1963**, *2*, 372.

(18) Selbin, J. J. *Chem. Rev.* **1965**, *65*, 153. Selbin, J. J. *Coord. Chem. Rev.* **1966**, *1*, 293.

(19) Cooper, S. R.; Koh, Y. B.; Raymond, K. N. *J. Am. Chem. Soc.* **1982**, *104*, 5092.

(20) Fisher, D. C.; Barclay-Peet, S. J.; Balfe, C. A.; Raymond, K. N. *Inorg. Chem.* **1989**, *28*, 4399.

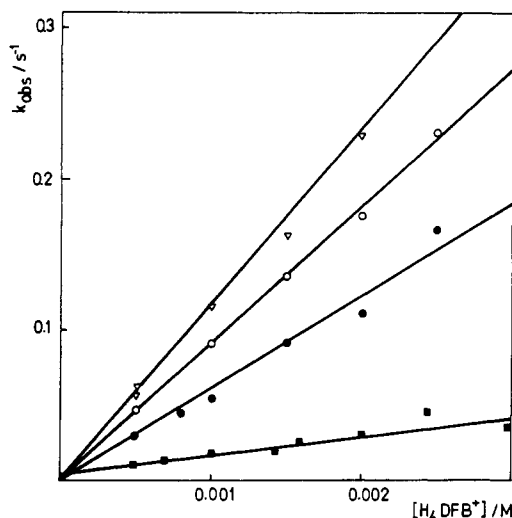


Figure 5. Dependence of the observed formation rate constant on the ligand concentration at 25 °C, 2.0 M ionic strength (perchlorate), and 510 nm. Conditions: $[\text{VOSO}_4] = 50 \mu\text{M}$; 1.6 mM HClO_4 (triangles); 16 mM HClO_4 (open circles); 0.16 M HClO_4 (full circles); 0.8 M HClO_4 (squares).

constant for the interconversion of the bidentate into the hexadentate complex (β_3/β_1), because no net proton is released during this interconversion. However, this equilibrium constant can be extracted from the kinetic data for this system (vide infra).

Kinetic Measurements. As mentioned in the experimental section, two types of kinetic experiments were performed, viz., the formation and hydrolysis of the produced complexes.

Figure 5 illustrates the dependence of the observed pseudo-first-order rate constant for the complexation of vanadyl ion with desferrioxamine B on the total concentration of the H_4DFB^+ ion (essentially the same rate constants are obtained independent of which one of the reactants is in excess). It is evident that the observed rate constant depends inversely on the proton concentration and linearly on the ligand concentration. The latter suggests that the rate-determining step of the studied reaction involves the formation of the bidentate complex, since a bimolecular interaction is only expected for this step (successive formation of the tetra- and the hexadentate complexes corresponds to the stepwise ring closing).

At a proton concentration lower than 0.16 M, zero intercepts are observed, since as predicted by the equilibrium measurements at these acidities the reverse hydrolysis reaction can then be completely neglected. At 0.8 M HClO_4 , "irreversibility" of the reaction is not ensured and an intercept is observed as expected from the equilibrium measurements.

In order to prevent the formation of any dimer in solution, a series of complex formation experiments were performed with the total concentration of the reactants as low as 5×10^{-5} M. Figure 6 demonstrates that the calculated forward rate constant multiplied by the proton concentration depends linearly on the proton concentration for $[\text{H}^+] \geq 0.05$ M. For this proton concentration range weighted *least-squares analysis* results in a slope and intercept of 16.9 (14) $\text{M}^{-1} \text{s}^{-1}$ and 2.55 (35) s^{-1} , respectively. The observed linearity can be explained by a simple reaction model that involves both the hydrolyzed and unhydrolyzed vanadyl-aquo ions as reactants with the H_4DFB^+ ion (vide infra the scheme). The deviations at $[\text{H}^+] < 0.05$ M could be due to a slight coupling of the first formation step with the consecutive ones, the third of which should exhibit an opposite proton dependence.

Consequently, the above results require that the analogous step for the backward reaction, i.e. the final hydrolysis step of the produced vanadyl-desferrioxamine B complex, should also proceed through proton-dependent and -independent pathways. Therefore, a series of experiments were performed in which the equilibrated, equimolar solution of VO^{2+} and H_4DFB^+ (in 2 M NaClO_4) was hydrolyzed against HClO_4 of various concentrations. Since at low acidity vanadium(IV) species easily undergo oxidation, vanadyl

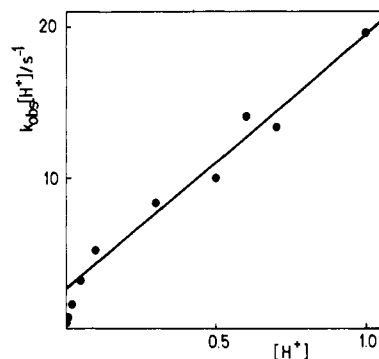


Figure 6. Dependence of the forward rate constant for the first formation step multiplied by the proton concentration on the proton concentration of the reaction solutions. Experimental conditions: $[\text{VOSO}_4]_0 = [\text{desferrioxamine B}]_0 = 50 \mu\text{M}$; 2.0 M ionic strength (perchlorate); at 25 °C; 510 nm.

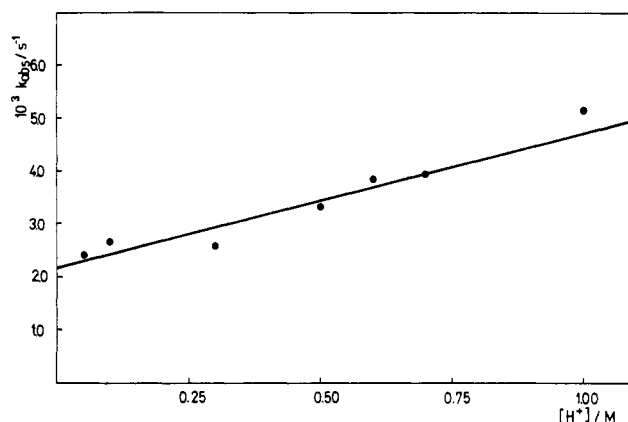


Figure 7. Dependence of the rate constant of the last (slowest) hydrolysis step of produced complex on the proton concentration of the reaction solutions. The experimental conditions are as for Figure 6.

sulfate was mixed with H_4DFB^+ in a deaerated perchlorate solution a few minutes before the pH jump was performed. The reaction proceeds through at least four distinct steps, the slowest one being accompanied by a decrease in absorbance at 510 nm and obviously corresponds to the reverse step of the studied formation reaction. This step was well separated on the time scale, and Figure 7 shows a linear dependence of the calculated hydrolysis rate constant (see Experimental Section for the integrated rate equation) on the proton concentration. A *least-squares analysis* results in a value of slope of 0.00256 (38) $\text{M}^{-1} \text{s}^{-1}$ and an intercept of 0.00219 (76) s^{-1} . The value of the slope for the forward reaction (Figure 6) divided by the slope of the reverse reaction (Figure 7) gives a value of 6601, which is in excellent agreement with the value of $K_1 = 6243$ determined via the spectrophotometric titration as described above. Under the employed experimental conditions, the second and third kinetic steps are much faster than the first one, and the rate expression that fully describes the kinetics of the first reaction step can be written as given in (7). The calculated values of the rate constants are summarized in Table I.

$$R = \{k_1 + k'_1 K_h [\text{H}^+]^{-1}\} [\text{VO}^{2+}] [\text{H}_4\text{DFB}^+] - \frac{k_{-1} [\text{H}^+] + k'_{-1}}{k_{-1} [\text{H}^+] + k'_{-1}} [(\text{H}_2\text{O})_3 \text{VO} (\text{H}_3\text{DFB})^{2+}] \quad (7)$$

The first three distinct steps of the hydrolysis process exhibit an increase in absorbance at 510 nm. Whereas the fastest one can be quite well separated, the second and third ones are too much coupled to be resolved. Figure 8 shows the dependence of the calculated rate constant of the fastest hydrolysis step on the proton concentration. It should be noted that the largest values of the observed rate constant approach the limits of the stopped-flow technique (the mixing-time of the instrument is approximately 3 ms) and are therefore determined with a quite large uncertainty. At low acidities the relaxation amplitudes are quite small. These

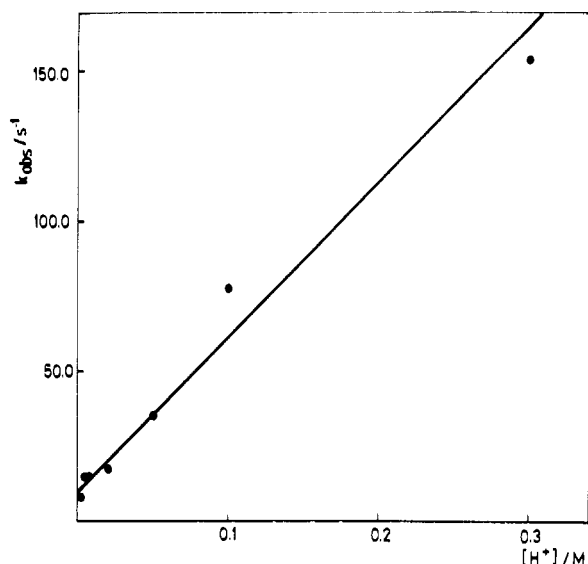


Figure 8. The first (fastest) hydrolysis rate constant of the produced complex plotted as a function of the proton concentration. The experimental conditions are as for Figure 6.

factors account for the deviations from linearity shown in Figure 8. The weighted *least-squares analysis* applied to the data results in a slope of $517 (62) \text{ M}^{-1} \text{ s}^{-1}$ and intercept of $10.3 (12) \text{ s}^{-1}$.

On the basis of the above mentioned arguments, it is reasonable to assume that mixing of VO^{2+} and H_4DFB^+ ions in sodium perchlorate ($[\text{H}^+] < 10^{-5} \text{ M}$) yields the tetradentate $\text{VO}(\text{H}_2\text{DFB})^+$ complex; hence the observed fast relaxation steps can be accommodated by the simplest reaction model that includes conversions of $\text{VO}(\text{H}_2\text{DFB})^+$ into $\text{VO}(\text{H}_3\text{DFB})^{2+}$ and $\text{V}(\text{HDFB})^{2+}$ (depending on the acidity of the reaction medium, in the slowest hydrolysis step the bidentate complex then eventually gives the free ligand and VO^{2+} ions). Since the dissociation of the oxo ligand is most probably a much slower process than the stepwise unwrapping of the hydroxamato group in the $\text{VO}(\text{H}_2\text{DFB})^+$ complex, the observed rate constant of the fastest hydrolysis step may be described in the simplest way by eq 8, where k_{-2} represents the rate

$$k_{\text{obs}} = k_{-2}[\text{H}^+] + k_2 \quad (8)$$

constant for the hydrolysis of $(\text{H}_2\text{O})\text{VO}(\text{H}_2\text{DFB})^+$ into $(\text{H}_2\text{O})_3\text{VO}(\text{H}_3\text{DFB})^{2+}$ and k_2 is its reverse. The ratio k_2/k_{-2} gives a value for the equilibrium constant K_2 defined by eq 3. If this equilibrium constant is combined with K_{II} from Table I, the value of $K_3 = K_{\text{II}}^{-1} - K_2^{-1}$ can also be calculated. Once K_2 and K_3 are known, these can be used to calculate $K_1 = K_{\text{I}}/(1 + K_2K_3)$. The calculated values of all of these constants are listed in Table I.

Discussion

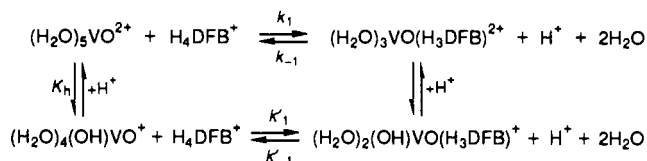
Our equilibrium measurements on the $\text{VO}^{2+}\text{-H}_4\text{DFB}^+$ system reveal high stability of the produced complexes. It is comparable to the stability of the complexes that this ligand forms with Fe(III),^{21,22} i.e. with the metal for which transport the siderophore is naturally produced. In strongly acidic media the stability of vanadyl complexes even exceeds the stability of the ferric complexes as a consequence of two facts: (i) In aqueous solutions under all conditions the hexadentate-bonded desferrioxamine B-vanadium(IV) complex is far more stable than the bidentate vanadyl complex ($\beta_3/\beta_1 = K_2K_3 = 333$). (ii) The oxo group of the vanadyl species on substitution by the ligand binds two protons to form a water molecule. Since this process is favored by high acidity, the hexadentate complex, from which the oxo ligand is expelled, also dominates over the tetradentate complex in acidic solutions. This in turn makes the vanadium ions competitive with iron(III) for desferrioxamine B in strongly acidic solutions, since

under such conditions ferrioxamine B exists only in the bi- and tetra- but not in the hexadentate form.

It is interesting to note that, although disputed, on many occasions the intravanadophoric milieu of the vanadocytes was reported to be strongly acidic, acidity being invoked only to preserve the V(III) and V(IV) states from oxidation (see ref 23 and citations therein).

Above $\text{p}[\text{H}^+] \sim 4$ in the complex that dominates the solutions desferrioxamine B is tetradentate bonded to the vanadyl ion without release of the oxo ligand, and the apparent stability constant of the desferrioxamine B-Fe(III) complex ($K_{\text{pH}=4} \sim 10^{15}$) greatly exceeds that of the vanadyl complex ($K_{\text{pH}=4} \sim 10^7$). Under these conditions only iron and not vanadium can form the hexadentate complex. Therefore, from our results, the hitherto known complexes, and their stability constants, no competition of vanadyl with iron(III) ions for desferrioxamine B at physiological acidities can be predicted.

The obtained kinetic results for the first formation (the slowest hydrolysis) step at $[\text{HClO}_4] \geq 0.05 \text{ M}$ can be accommodated by the two parallel path mechanism outlined in the following scheme:



From the values in Table I, assuming $K_h = 1.1 \times 10^{-6}$,²⁴ a rather high ratio of $k'_1/k_1 \sim 10^5$ can be calculated. This is 2 orders of magnitude larger than the one obtained for the analogous pathways of iron(III)²² and 10 times larger than that for aluminum(III)²⁵ ions. For the latter two metal ions the effect was explained in terms of the reduction of the positive charge on the metal ions and the labilization of the coordinated water molecules by the hydroxo ligand. An equatorial water molecule that must be expelled from the vanadyl ion in order to coordinate a bidentate ligand, such as an hydroxamato group of the H_4DFB^+ ion, exchanges with a rate constant of ca. 500 s^{-1} ,²⁶ and its exchange rate must also be increased by such a labilization effect. However, it was suggested²⁷ that the labilizing effect of the hydroxo group on the water molecule of the vanadyl ion should not exceed the effect observed for iron(III) and aluminum(III) ions, which are 3+ charged species, whereas the vanadyl ion experiences less positive charge.²⁸ A plausible explanation of this effect can therefore not be based on this simple model.

For the chelation of iron(III) by hydroxamates, Crumbliss and co-workers²⁹ proposed formation of a hydrogen bond between the ligand and the solvated metal ions. This can also be applied to the vanadyl ion with the oxo and hydroxo ligands in a cis position. The strongly polar complex should be able to donate its electron density toward the proton of the terminal ammonium or the hydroxamato group of the H_4DFB^+ ion.

An alternative explanation can be based on the model given by Johnson and Murmann.³⁰ They studied the kinetics of the exchange of the vanadyl oxo ligand in water and obtained an analogous ratio of $k'_1/k_1 = 6 \times 10^4$. The authors explained their results by proposing a low-energy pathway in which the oxo and hydroxo ligands mutually interconvert through an oxygen equivalence in the activated state. This model is also applicable in our case, since this effect could modify the equatorial water molecules into those more similar to the axial one. This should

(23) Frank, P.; Carlson, R. M. K.; Hodgson, K. O. *Inorg. Chem.* **1986**, *25*, 470.

(24) K_h at 25 °C and 2.0 M ionic strength was calculated using the expression given in: Baes, C.; Mesmer, P. *Hydrolysis of Cations*; Wiley: New York, 1967.

(25) Garrison, J. M.; Crumbliss, A. L. *Inorg. Chim. Acta* **1987**, *138*, 61.

(26) Wuthrich, K.; Connick, R. K. *Inorg. Chem.* **1975**, *14*, 2895.

(27) Che, T. M.; Kustin, K. *Inorg. Chem.* **1980**, *19*, 2275.

(28) Ballhausen, C. J.; Gray, H. B. *Inorg. Chem.* **1962**, *1*, 111.

(29) Monzyk, B.; Crumbliss, A. L. *J. Am. Chem. Soc.* **1979**, *101*, 6203.

Brink, C. P.; Crumbliss, A. L. *Inorg. Chem.* **1984**, *23*, 4708.

(30) Johnson, M. D.; Murmann, R. K. *Inorg. Chem.* **1983**, *22*, 1068.

(21) Monzyk, B.; Crumbliss, A. L. *J. Am. Chem. Soc.* **1982**, *104*, 4921.

(22) Biruš, M.; Bradić, Z.; Krznarić, G.; Kujundžić, N.; Pribanić, M.; Wilkins, P. C.; Wilkins, R. G. *Inorg. Chem.* **1987**, *26*, 1000.

make the exchange rate about 10^5 – 10^8 times faster, since the axial water molecule exchanges with a rate constant of $\sim 10^8$ s $^{-1}$.²⁶ The fact that both $(\text{H}_2\text{O})_4(\text{OH})\text{VO}^+$ and $(\text{H}_2\text{O})_4\text{VO}_2^{+6}$ react with H_4DFB^+ with approximately equal rate constants (1×10^5 M $^{-1}$ s $^{-1}$ and 2.3×10^5 M $^{-1}$ s $^{-1}$, respectively) makes this model more attractive than the one involving formation of hydrogen bonds.

It is generally accepted that the inner-sphere substitution reactions proceed via a mechanism in which the formation of an outer-sphere complex precedes the rate-determining step. The formation rate constant is defined as $k_f = k_{\text{ex}}K_{\text{out}}$, where k_{ex} and K_{out} are the water-exchange rate constant and the outer-sphere complex stability constant, respectively. K_{out} can be calculated according to the Eigen–Fuoss equation³¹ for (2+,1+) interaction. However, H_4DFB^+ is a large and nonspherical ion, making an estimation of the closest approach of the reacting species very uncertain and the calculated value of K_{out} unreliable. On the other hand, K_{out} for the $\text{Fe}(\text{H}_2\text{O})_5\text{OH}^{2+}$ – H_4DFB^+ outer-sphere complex can be calculated easily as $k_f/k_{\text{ex}} = 3.6 \times 10^3/1.2 \times 10^5 = 3 \times 10^{-2}$ M $^{-1}$.^{22,32} Since the hydroxoiron(III) and vanadyl ions are equally charged, their outer-sphere stability constants should not differ significantly. Therefore, this value of K_{out} and k_1 given in Table I can be used for calculation of water-exchange rate constants of vanadyl ion, which then can be compared to the experimental value. The calculated value of $k_{\text{ex}} = k_1/K_{\text{out}} = 563$ s $^{-1}$ favorably compares to the experimental $k_{\text{ex}} = 500$ s $^{-1}$.²⁶ This suggests that the substitution of a water molecule by H_4DFB^+ on these two metal ions follows the same dissociative mechanism

because their rates appear to be dominated by the water exchange. Unfortunately, a lack of relevant data for the water exchange on $(\text{H}_2\text{O})_4\text{VO}(\text{OH})^+$ makes a similar analysis for this ion impossible.

Che and Kustin²⁷ reported a much smaller effect of the hydroxo ligand for the complex formation kinetics of vanadyl ion with a series of bidentate ligands than what we observed for H_4DFB^+ . However, it should be noted that the experimental conditions used in these two studies are very different (they worked at pH ranging from 3 to 4.5 but at much higher vanadyl concentrations where dimerization of vanadyl ion cannot be excluded).

The kinetic steps that follow the initial formation of the bidentate complex are faster and were studied only for the hydrolysis of the produced complex. The fastest and kinetically well-resolved step was attributed to the formation of the bidentate complex by the hydrolysis of the tetradentate complex. Even though it is dangerous to compare the kinetics of the asymmetric vanadyl ion with the kinetics of the symmetric Fe(III) ion, the obtained values of the hydrolysis rate constants of the tetradentate-bound complexes of these two metal ions confirm that the assignment of the kinetic step is reasonable. The unwrapping of the ferri tetradentate complex appears to be ca. 50 times slower than that of the analogous vanadyl complex. This is qualitatively what one may expect considering the effect of the coordinated oxo group on the charge of the central metal ion and in turn on the kinetic stability of its desferrioxamine B complex.

Acknowledgment. We thank Prof. R. G. Wilkins for using the rapid-scan facilities at the New Mexico State University and Dr. V. Nöthig-Laslo from the “Rudjer Bošković Institute”, Zagreb, for recording the ESR spectra. This work received financial support from the Croatian Fund for Research, which is gratefully acknowledged.

(31) Eigen, M. Z. *Phys. Chem. (Frankfurt)* 1954, 1, 176. Fuoss, R. M. J. *Am. Chem. Soc.* 1958, 80, 5059.

(32) Swadle, T. W.; Merbach, A. E. *Inorg. Chem.* 1981, 20, 4212.

Contribution from the Department of Macromolecular Science, Faculty of Science, Osaka University, Toyonaka, Osaka 560, Japan

Influence of the Distal Para Substituent through NH---S Hydrogen Bonds on the Positive Shift of the Reduction Potentials of $[\text{Fe}_4\text{S}_4(\text{Z-cys-Gly-NHC}_6\text{H}_4\text{-}p\text{-X})_4]^{2-}$ (X = H, OMe, F, Cl, CN) Complexes

Ryotaro Ohno, Norikazu Ueyama, and Akira Nakamura*

Received February 5, 1991

$[\text{Fe}_4\text{S}_4(\text{Z-cys-Gly-NHC}_6\text{H}_4\text{-}p\text{-X})_4]^{2-}$ (X = H, OMe, F, Cl, CN) complexes were prepared as models of *P. aerogenes* ferredoxin, whose redox potential is controlled by NH---S hydrogen bonds. Their reduction potentials became more positive in CH_2Cl_2 at 298 K as the electron-withdrawing tendency of the substituent increased. The most positive potential was observed at -0.80 V vs SCE for the 3–/2– couple of $[\text{Fe}_4\text{S}_4(\text{Z-cys-Gly-NHC}_6\text{H}_4\text{-}p\text{-CN})_4]^{2-}$ (1), in which all of the amide NH of an anilide residue participated in intramolecular NH---S hydrogen bonds probably with a cysteinyl sulfur atom. The reduction potential of 1 controlled by the electronic property of its ligand was -1.13 V vs SCE.

Introduction

Ferredoxins have the function of electron transfer and are characterized by a cluster consisting of four iron atoms coordinated by four inorganic sulfide ions and thiolate groups of cysteine residues.¹ One important aspect of ferredoxin research has been the elucidation of controlling factors of the reduction potential.

Holm and his co-workers have extensively investigated the reduction potentials of $(\text{Fe}_4\text{S}_4)^{2+}$ ferredoxin model complexes with alkane- and arenethiolato ligands and found that not only the dielectric constant of a solvent^{2,3} but also the electronic property of a ligand³ exerted influences on the reduction potentials of

$(\text{Fe}_4\text{S}_4)^{2+}$ complexes. However, reduction potentials of their model complexes were far more negative than those of native ferredoxins.¹

On the other hand, it has been proposed that NH---S hydrogen bonds are the major mechanism of influence of a polypeptide on reduction potentials of ferredoxins as evidenced by the X-ray analysis of *P. aerogenes* ferredoxin.⁴ Actually, we experimentally verified the influence of NH---S hydrogen bonds on the reduction potential using ferredoxin model complexes with tripeptide ligands containing a sequence Cys-Gly-Ala, which was characteristic of *P. aerogenes* ferredoxin.⁵ Reduction potentials of $[\text{Fe}_4\text{S}_4(\text{Z-cys-Gly-Ala-OMe})_4]^{2-6}$ (Z = benzyloxycarbonyl) and $[\text{Fe}_4\text{S}_4(\text{Z-cys-Gly-Ala-cys-OMe})_2]^{2-}$ shifted positively in CH_2Cl_2 at low temperature, where NH---S hydrogen bonds from NH of the Ala

(1) Berg, J. M.; Holm, R. H. *Iron-Sulfur Proteins*. In *Metal Ions in Biology*; Spiro, T. G., Ed.; Wiley-Interscience: New York, 1982; Vol. 4, p 1.

(2) Hill, C. L.; Renaud, J.; Holm, R. H.; Mortenson, L. E. *J. Am. Chem. Soc.* 1977, 99, 2549.

(3) DePamphilis, B. V.; Averill, B. A.; Herskovitz, T.; Que, L., Jr.; Holm, R. H. *J. Am. Chem. Soc.* 1974, 96, 4159.

(4) Carter, C. W. *J. Biol. Chem.* 1977, 252, 7802.

(5) (a) Ueyama, N.; Terakawa, T.; Nakata, M.; Nakamura, A. *J. Am. Chem. Soc.* 1983, 105, 7098. (b) Ueyama, N.; Kajiwara, A.; Terakawa, T.; Ueno, T.; Nakamura, A. *Inorg. Chem.* 1985, 24, 4700.

(6) Small letter cys represents Cys residue coordinating to Fe ion.